The Statistical Properties of a Zonal Jet in a Baroclinic Atmosphere: A Semilinear Approach. Part I: Quasi-geostrophic, Two-Layer Model Atmosphere

A. SPERANZA AND P. MALGUZZI

CNR-FISBAT, Bologna

(Manuscript received 22 May 1987, in final form 11 March 1988)

ABSTRACT

A semilinear (the wave-dynamics are linear with the time-evolution operator determined by the time-varying zonal flow while the zonal flow is fully nonlinear in the eddy fluxes) model of a baroclinic zonal jet is integrated, under macroscopic conditions realistic for the earth's atmosphere, for a time period of 20 years in a high resolution pseudospectral version and its asymptotic (in time) statistical properties are determined.

The model is studied as a dynamical system, both by following sequences of bifurcations from the stable Hadley circulation and by embedding in lower dimension spaces. The model turns out to be far from amenable to weakly nonlinear approximations common in atmospheric and oceanographic literature.

The analysis of propagation of disturbances in the turbulent jet demonstrates the inadequacy of mean-field approximations usually adopted in studies of kinematics of Rossby waves, teleconnections, etc.

1. Introduction

Ever since the role of nonsymmetric disturbances in maintaining the observed zonal circulation was recognized (Defant 1921; Jeffreys 1926; Douglas 1931), the problem of setting up a consistent physical theory of the interaction between an appropriate (time or zonal or ensemble) average flow and deviations from it has been central in meteorology (Saltzman 1968; Saltzman and Vernekar 1968, 1971; for recent summaries see Saltzman 1978; Hoskins 1983).

Unfortunately, the earth's atmosphere displays no clear-cut space–time scale separation. This circumstance makes the task of computing averages and describing their dynamics a difficult one, and it comes as no surprise that success has as yet not been achieved. The situation is the same in all branches of fluid dynamics where similar problems have been approached. In this respect we quote, after Hussain (1983): ". . . even though many researchers have suggested instability to be that of the local mean profile, this author feels that the instantaneous dynamics must control the instability. The instantaneous profile in a turbulent shear flow seldom resembles the time-mean profile, from which it departs wildly. That is, a disturbance never sees the mean profile. Since instability is sensitive to the details of the profile, it is hard to understand how an instability analysis based on the mean profile can explain. . . . The flow being highly time dependent, instability analysis of a static mean profile seems hardly relevant. . . ."

However, the theory of dynamical systems, developed after the pioneering efforts of E. Lorenz, provides clear exemplifications of the technical reasons for the failure of the averaging approximation (see, for example, Farmer 1982). Unfortunately, the extrapolation of dynamical system theory to the limit of continuous field equations is still not clear.

In this paper we shall reconsider the whole matter by developing a set of field equations that are complex enough to display "earthlike"[1] atmospheric behavior, but simple enough to allow a thorough statistical study by numerical integration with an adequate computer. We confine our study to quasi-geostrophic, two-layer equations; in view of the methodological nature of the paper this limitation should not be taken too seriously. We will derive our field equations on the basis of the zonal symmetry of the physical system and "shape" assumptions for the disturbances (a definition of the concepts and terminology used here can be found in Hart 1979). Zonal averages could be substituted with any other average (see, again, Hoskins 1983) and the "shape" assumption is no more than a parameterization of nonlinearity of the field equations.

Once the model is described (section 2), we present some statistical properties resulting from a long-term numerical integration (section 3) for a parameter setting yielding fully developed chaotic behavior. Our ap-

Corresponding author address: Dr. P. Malguzzi, Dinamica Atmosferica, CNR-FISBAT, % Dipartimento de Fisica, Via Irnerio 46, I-40126 Bologna, Italy.

[1] Earthlike means, for our purposes, that the predicted variables in our model show chaotic behavior with unimodal probability density distribution.

proach is to consider the general statistical properties of our model atmosphere and to try to develop a (possibly simple) theory capable of explaining the properties of the model's general circulation in the chaotic regime. After careful examination of the literature available on this subject, it seems that the most popular theory relates some properties of the general circulation (like heat and momentum fluxes) to those of the most unstable normal mode of the eigenvalue problem arising from linearization of the governing equations around the climatological-mean state. (See, for example, Simmons and Hoskins 1978; Frederiksen 1978, and the recent surge of works on the stabilizing effect that dissipation has on baroclinic instability.) Since the time-mean state is not an exact, stationary solution of the governing equations, it is common practice to assume the existence of an "ad hoc" external forcing which renders this state as a fixed point. In section 4 we test this classical "mean field" approximation for both homogeneous and nonhomogeneous (thermally forced) circulations, pointing out the main inconsistencies of such an approximation.

We next examine (section 5) other possible approaches to the problem, such as following the bifurcation sequence leading to chaos or trying several low-order models obtained by severely truncating our model atmosphere. Following the classical work of Pedlosky (1970), an attempt is made to relate the chaotic behavior with some periodic (or quasi-periodic) orbits lying in the same region of the phase space as the attractor of the complete system. This procedure turns out to be useless for the case described herein. In section 6, we draw our conclusions.

2. The model

The model used in the numerical experiments discussed herein is deduced from the two-layer, quasi-geostrophic equations:

$$\partial_t \nabla^2\phi + J(\phi, \nabla^2\phi + \beta y) + J(\tau, \nabla^2\tau) = -\frac{\nu_E}{2}\nabla^2(\phi - \tau) \quad (1)$$

$$\partial_t(\nabla^2\tau - 2F\tau) + J(\tau, \nabla^2\phi + \beta y) + J(\phi, \nabla^2\tau) = \frac{\nu_E}{2}\nabla^2(\phi - \tau) - \nu_S\nabla^2\tau + 2F\nu_H(\tau - \tau^*). \quad (2)$$

Here $\phi = (\psi_1 + \psi_3)/2$ and $\tau = (\psi_1 - \psi_3)/2$ are, respectively, the barotropic and the baroclinic (temperature) components of the streamfunction ψ; J, the Jacobian operator; ∇^2, the Laplacian operator; F, the Froude number; ν_E, ν_S, and ν_H are, respectively, the coefficients of Ekman pumping at the lower surface, friction at the surface separating the two layers, and Newtonian cooling; β, the gradient of the Coriolis parameter; and τ^*, the baroclinic generation which forces the fluid motion (see, for instance, Lorenz 1963). The variables are in the standard nondimensional form of Pedlosky (1979).

After separating the zonally symmetric part of the vertically averaged velocity and vertical shear $U(y, t)$ and $m(y, t)$ respectively:

$$\phi = -\int U(y, t)dy + \phi'(x, y, t) \quad (3)$$

$$\tau = -\int m(y, t)dy + \tau'(x, y, t). \quad (4)$$

We introduce a particular form of the solution for the nonsymmetric component:

$$\phi' = \sum_n A_n(y, t)g_n(x)\cdots + (*) \quad (5)$$

$$\tau' = \sum_n B_n(y, t)g_n(x)\cdots + (*) \quad (6)$$

where "$(*)$" indicates the complex conjugate of the preceding term, and the separated x-structure functions $g_n(x)$ are assumed "ad hoc". The main advantage of such representation consists in the fact that projection of the equations of motion onto the (complete) $\{g_n\}$-basis gives coefficients of nonlinear interaction that can be made to assume opportune numerical values by properly choosing the g_n's. Here we concentrate on the simplest case:

$$\left.\begin{aligned} g_1(x) &= e^{i\kappa x} \\ g_n(x) &= 0, \quad n > 1 \end{aligned}\right\} \quad (7)$$

that, as we shall see, is sufficient to produce an "essential" dynamics of maintenance of the middle latitude jet. As already pointed out in the Introduction, by "essential" we mean that the degrees of freedom of the model must show, for a realistic range of the external parameters, chaotic behavior with unimodal probability density distribution. With assumptions (7), Eqs. (3) and (4) reduce to

$$\phi = -\int U dy + Ae^{i\kappa x} + (*)$$

$$\tau = -\int m dy + Be^{i\kappa x} + (*)$$

and, by projection of (1) and (2) onto $g_1(x)$ we obtain

$$\dot{U} + \frac{\nu_E}{2}(U - m) + 2\kappa\,\mathrm{Im}\{AA^*_{yy} + BB^*_{yy}\} = 0 \quad (8)$$

$$\dot{m}_{yy} - 2F\dot{m} + \nu_S m_{yy} - \frac{\nu_E}{2}(U - m)_{yy} - 2F\nu_H(m - m^*) + 4\kappa\,\mathrm{Im}\{A^*B\}_{yy} + 2\kappa\,\mathrm{Im}\{AB^*_y + BA^*_y\}_{yyy} = 0 \quad (9)$$

$$\dot{A}_{yy} - \kappa^2\dot{A} + (\nu_E/2 + i\kappa U)A_{yy} - \left[i\kappa^3 U + i\kappa U_{yy} - i\kappa\beta + \frac{\nu_E}{2}\kappa^2\right]A - \left(i\kappa m_{yy} - i\kappa^3 m - \nu_E\frac{\kappa^2}{2}\right)B + \left(i\kappa m - \frac{\nu_E}{2}\right)B_{yy} = 0 \quad (10)$$

$$\dot{B}_{yy} - \kappa^2\dot{B} - 2F\dot{B} + \left(\frac{\nu_E}{2} + \nu_S + i\kappa U\right)B_{yy} - \left[i\kappa^3 U - i\kappa\beta + i\kappa U_{yy} + \frac{\nu_E}{2}\kappa^2\right]B + [\nu_S\kappa^2 + 2F\nu_H + 2i\kappa FU]B - \left(i\kappa m_{yy} + i\kappa^3 m - \nu_E\frac{\kappa^2}{2} - 2i\kappa Fm\right)A + \left(i\kappa m - \frac{\nu_E}{2}\right)A_{yy} = 0 \quad (11)$$

where

$$\tau^* = -\int m^*(y)dy$$

and where, because of the simple wavelike form of the nonsymmetric disturbances in (7), all the wave–wave interaction coefficients vanish and the only nonlinear interactions take place between symmetric and nonsymmetric components (latitudinal convergence of eddy momentum flux and heat flux). Equations (8)–(11) constitute a set of six real field equations in latitude y and time t with coefficients A and B being complex. We will assume as lateral boundary conditions rigid walls at $y = 0, L_y$, which imply $U = m = A = B = 0$ at the boundaries. System (8)–(11) can be transformed into a set of ordinary differential equations by further decomposing U, m, A, B in Fourier series:

$$\begin{pmatrix} U \\ m \\ A \\ B \end{pmatrix} = \sum_{J=1}^{JT} \begin{pmatrix} U_J \\ m_J \\ A_J \\ B_J \end{pmatrix} \sin\left(\frac{\pi Jy}{L_y}\right).$$

Such decomposition, performed using standard techniques, is not discussed here. The system is driven in Eq. (9) for the vertical shear through the term $2F\nu_H(m - m^*)$ which forces a relaxation to the radiative equilibrium $m^*(y)$. In the following, the radiative equilibrium potential temperature profile will be assumed with the form

$$\theta^* = 2\tau^* = \theta_E \cos\left(\frac{\pi y}{L_y}\right)$$

which corresponds to the vertical shear

$$m^* = \theta_E \frac{\pi}{2L_y} \sin\left(\frac{\pi y}{L_y}\right).$$

The parameter θ_E (representing half of the equator-to-pole temperature contrast at the radiative equilibrium) will be determined empirically in such a way as to give the desired behavior of our model atmosphere (see Malguzzi–Speranza 1986, for a comparison with observations).

System (8)–(11) describes the nonlinear equilibration of a single baroclinic wave through interactions with the zonal component. In section 3 we discuss the statistical properties of such equilibration in the highly supercritical regime. We shall see that a "turbulent" zonal jet is maintained by the process modeled by (8)–(11).

3. Statistical properties: The "general circulation" of the model

In this section we illustrate the statistical properties of the model atmosphere described in section 2 with the purpose of justifying its use in order to test some methodological hypotheses of the classical theory of general circulation.

Numerical integrations of the system (8)–(11) have been performed with the spectral scheme discussed in section 2 at different levels of resolution. The experiments discussed here have been run with a leapfrog scheme (time step $\frac{1}{200}$ day) for the time derivative and a pseudospectral representation with 32 Fourier modes in latitude. The computational mode is damped by suitably averaging in time the variables every 20 time steps. The integration is carried on for 1 280 000 time steps corresponding to 20 yr of real time. Dissipation coefficients are fixed to the values $\nu_E = 0.45$ (that spins down the whole atmosphere with a decay time of 5 days) and $\nu_S = \nu_H = 0.1157$ (decay time 10 days). Other parameters are $F = 2$, $\beta = 1.6$, $k = 1.3$ (wavelength $\approx$ 4800 km), and $L_y = 10$ (10 000 km). The external forcing, acting only on the gravest latitudinal

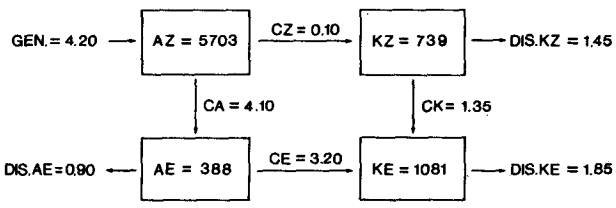

FIG. 1. Energy cycle averaged over 20 yr for the experiment described in section 3. Units are w m^{-2} for energy conversions and 1000 J m^{-2} for energy contents. Here, AZ, AE, KZ, KE refer, respectively, to available energy of the zonal flow, available energy of the eddy part, kinetic energy of the zonal flow, and kinetic energy of the eddies.

mode, is $\theta_E = 9$ (equator to pole temperature difference of 54 K at radiative equilibrium). This value turns out to give (having fixed the other parameters) a superrotation (mean westerly momentum) of 6.8 m s^{-1} which we consider typical of the winter circulation.

Visual inspection at different fields reveals that the life cycle of nonsymmetric disturbances is characterized by baroclinic growth and barotropic momentum convergence into the jet. Also, the symmetric component evolves in a reasonable fashion: all the classical schemes of maintenance of the midlatitudinal jet are respected, as shown by the energy diagram of Fig. 1. In fact, the comparison of Fig. 1 with Lorenz (1967) is quite satisfactory given the simplicity of the model considered (CK and DIS.KZ are overestimated here).

Figure 2 displays, for the lowest zonal and wave components, the scatter of states sequentially occupied by the system in time. Figure 3 shows the specific probability densities. Figure 4 shows the average in time (over 20 years) of the zonal flow, revealing a high degree

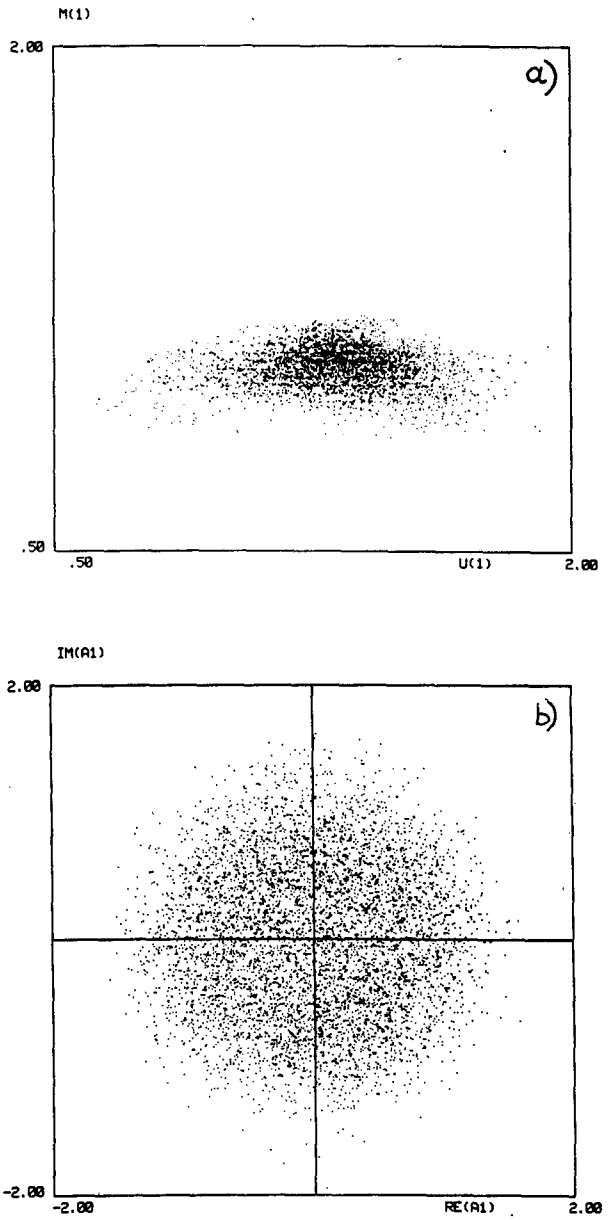

FIG. 2. (a) Scatter diagram of the first meridional component of zonal wind shear (m_1) versus the first component of the zonal wind (U_1). Units are dimensionless (one unit corresponds to 10 m s^{-1} for the wind components and 100 m of geopotential for the wave components). The total time of integration is 20 years. (b) as in (a) but for the real and imaginary parts of the first barotropic meridional component of the wave field (A_1).

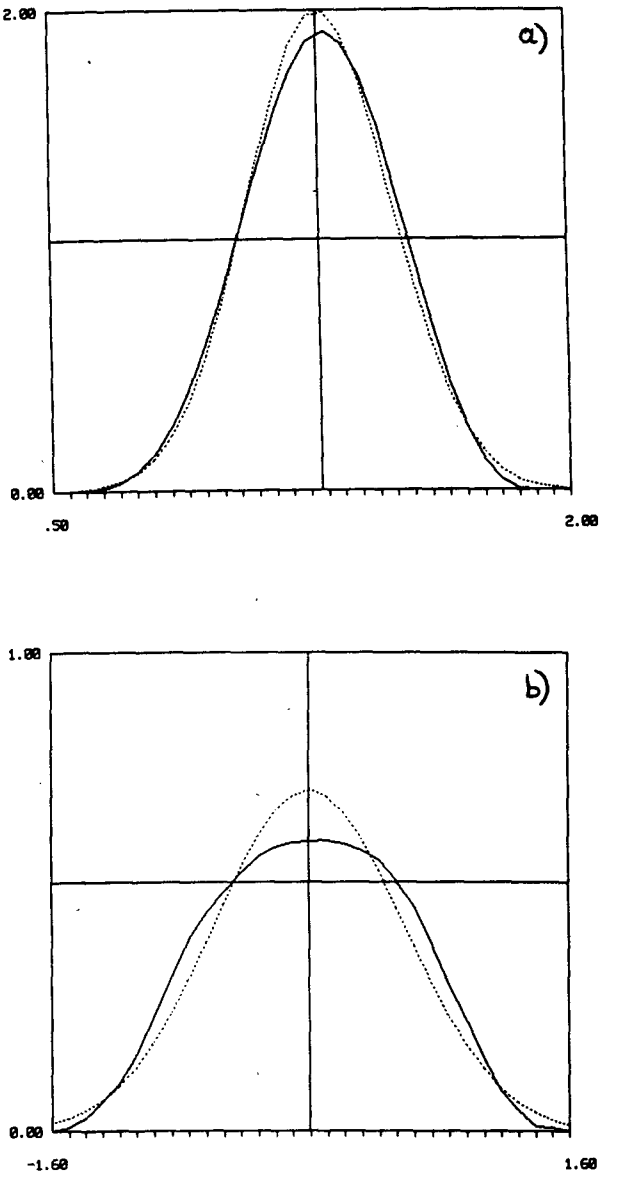

FIG. 3. (a) Histograms of U_1 (solid line). The dashed line represents a gaussian having the same mean and variance as the distribution of U_1. (b) as in (a) but for the real part of A_1.

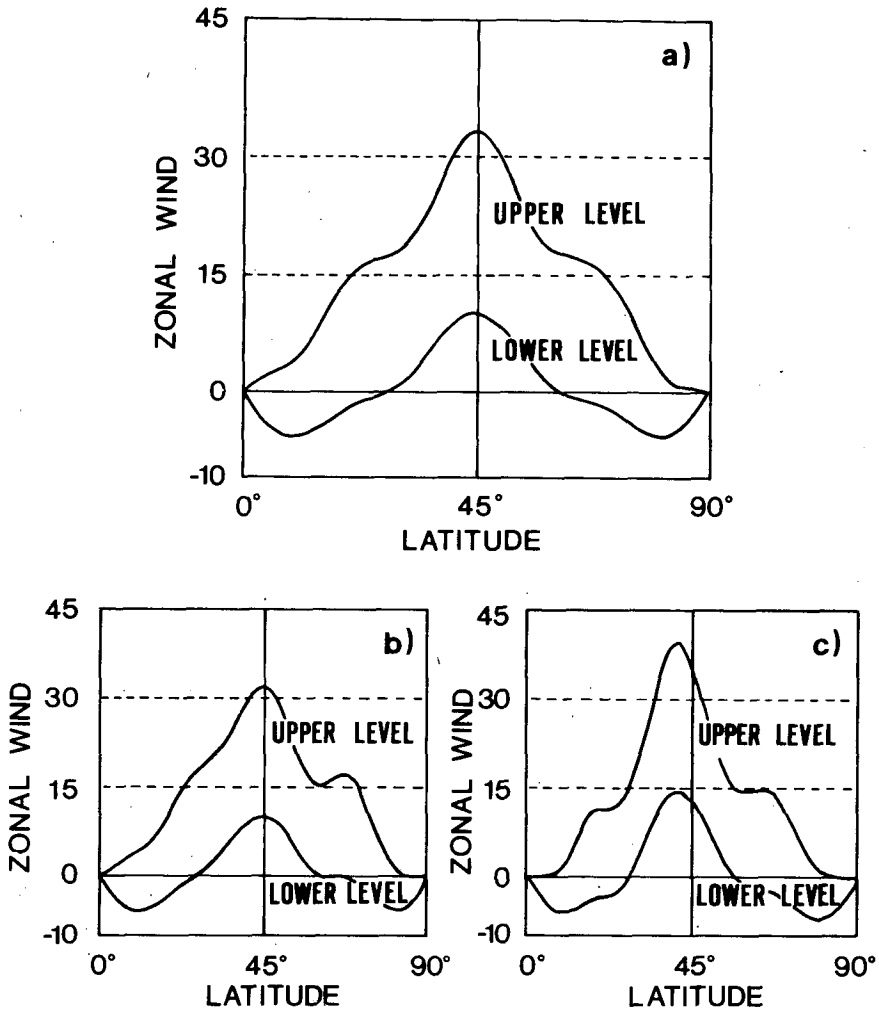

FIG. 4. (a) The 20 yr average of the zonal wind versus latitude at the upper level (lev. 1) and lower level (lev. 3). Units are m s^{-1}. Examples of averages over individual years are shown in panels (b) and (c).

of variability from year to year (Fig. 4b and 4c). The average of wave amplitude tends obviously to zero. The power spectra, shown in Fig. 5, confirm the chaotic nature of the system. Combined wavenumber–frequency spectra reveal the energetic dominance of the lowest harmonics (Fig. 6).

Inspection of the system reveals that the statistical properties of the jet and the associated waves are earth-like. The model atmosphere described above meets the requirements for a study of the zonal circulation properties in a chaotic, baroclinic regime since it displays the desired statistical behavior, although maintaining the dimensionality low enough to allow thorough numerical analysis.

4. A reexamination of the classical formulation of the theory of general circulation

The classical theory of general atmospheric circulation revolves around the idea that turbulent fluxes maintain an "equilibrium circulation", i.e., the time-mean circulation, which is remarkably different from the *true* stationary solution (the so-called Hadley circulation). Dynamical theories of fluctuations produced in the above context, typically based on linear stability analysis, usually refer to such a time mean state, considered as a stationary solution.

In order to exemplify the dangers involved in a naive application of averaging procedures, we will test the consistency of the classical theoretical framework by analyzing our model atmosphere on the basis of the "equilibrium" circulation as approximated by the average zonal flow of Fig. 4a. Linear stability analysis of this circulation gives the results shown in Fig. 7. As expected, the system is pushed by heat and momentum fluxes quite near to marginal stability, although still remaining within the unstable range. To highlight the inconsistencies encountered in the formulation of a theory along the lines of traditional meteorology, we

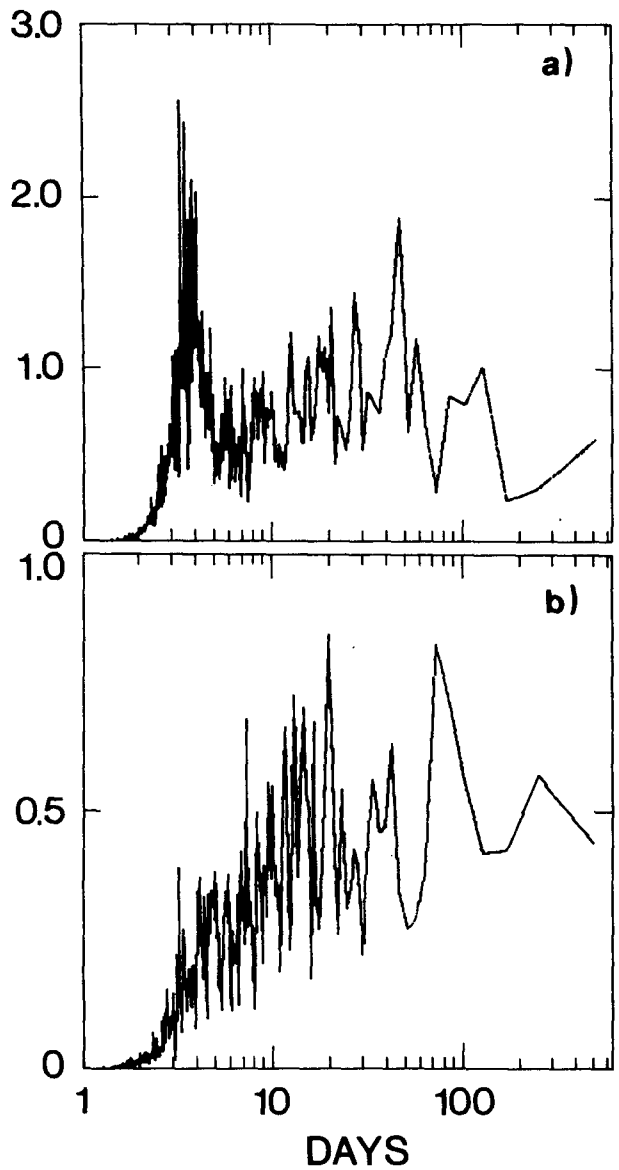

FIG. 5. Power spectrum of (a) real part of A_1, and (b) real part of A_2. In the abscissa, the period (in days) is on the logarithmic scale.

resorted to a numerical experiment, thus avoiding the laborious computations typical of weakly nonlinear expansions. The experiment consisted of a 10-yr numerical integration of the system (8)–(11) for a choice of the external forcing that balances the time-mean state. As a consequence the new system has a fixed point exactly in the maximum frequency state. The scatter diagrams of various components are reported in Fig. 8. Comparison with the statistics of the original experiment (see again Fig. 2) reveals two conspicuous problems: the variance is too small and the new statistical equilibrium is shifted with respect to the old one. The first problem is associated with the circumstance that the system is very near to marginal stability of the time-mean state. Theoretically, this problem can be handled by carefully reshaping the center manifold near marginal stability with the introduction of new terms in the equations. Thus, the need for an accurate rewriting (renormalization) of the equations again emerges.

But it is in the second problem that the physical nature of the limitations of classical theory appears most clearly: the shift of the equilibrium is caused by an essential symmetry of the system, namely that associated with the property of baroclinic instability to transport heat only in one latitudinal direction so that nothing like an "antibaroclinic" instability exists. As a consequence, average baroclinicity can only decrease. One is easily convinced that this difficulty must be faced no matter how one modifies the stability problem; it is not model-dependent and is, therefore, basic.

The existence of a most probable (central) state is due to the existence of several statistically independent processes that produce a centered statistics in the sense of the central limit theorem. The central state has no special dynamical meaning and carries no special information regarding the dynamics of the fluctuations. The reduction to a minimal system of low dimensionality, if any, must be made by choosing the basic modes in a more elaborate fashion. (See the discussion of this problem in section 5). Therefore, the foundations of the theory of general circulation appear rather shaky. *This explains, perhaps, why it is so often invoked, but seldom thoroughly formulated!*

In order to cast more light on the faults of classical approaches, we examine another aspect of the general circulation, namely computations of anomalies forced by "tropical" heat sources, in which the time-mean state is used to infer statistical properties regarding the circulation. A model like the one described in section 2 is clearly inadequate to describe tropical dynamics, however, as already mentioned, the point we debate here is methodological: Can we compute the response to tropical heating in terms of linear or nonlinear deviations with respect to a static "basic state"?

Our answer to this question is negative. The physical motivations of this negative response have been, in essence, already outlined: the time mean state is simply the result of a central limit statistical accumulation on a most probable state and is not characterized by any particular dynamical property. Direct evidence of the significance of our criticism of the classical approach is provided in terms of a numerical experiment performed with the model described in section 2.

In order to simulate anomalous tropical heating we insert in our model a nonsymmetric, stationary heat source $-FH(x, y)$ in the right-hand side of (2) having the structure:

$$H = H_0 e^{-(y-y_H)^2} e^{ikx} \qquad (12)$$

where $H_0 = 0.5$ (heating rate of 3 K day^{-1}) and

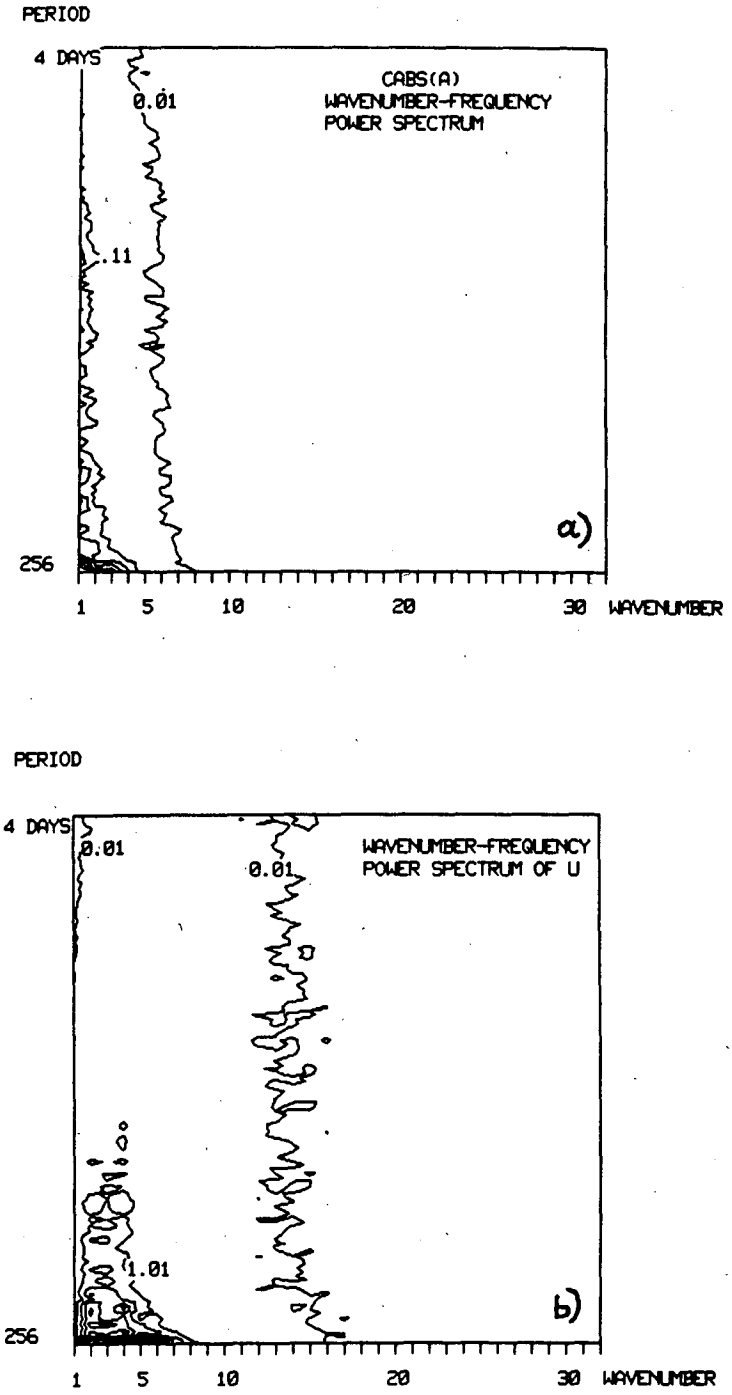

FIG. 6. Wavenumber–frequency power spectrum for (a) barotropic wave-component A (contour interval 0.1) and (b) zonal wind U (contour interval 1). On the y-axis, the period is on the logarithmic scale and on the x-axis, the meridional wavenumber.

$y_H = 2$. The latitudinal structure of the "tropical" heat source (a localized Gaussian) is shown in Fig. 9.

The addition of such a source is capable of modifying the climate of our model, although not to any great extent. This is shown in Fig. 10 displaying the time-mean flow (10a) and the time-mean anomaly (10b); despite the strong internal heat source, the 10 yr average anomaly at the ground is about 1 mb. The disturbance

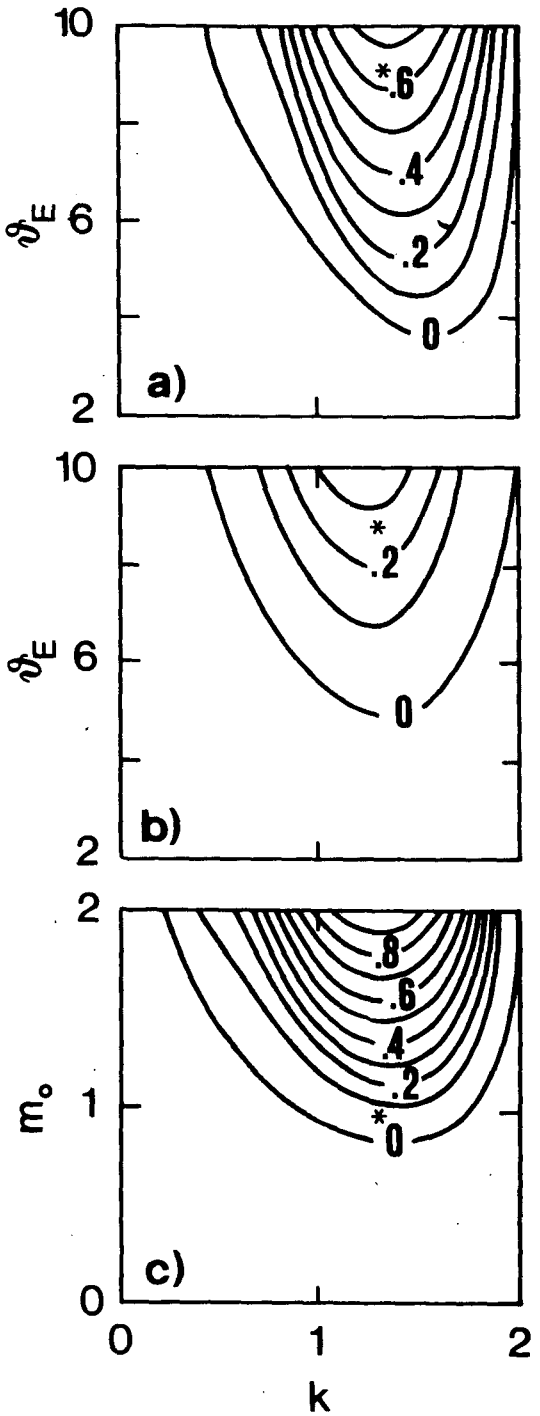

FIG. 7. Growth rates of (a) the most unstable, symmetric, and (b) antisymmetric eigenmodes of the linear stability analysis of the Hadley circulation versus the zonal wavenumber k and the external forcing θ_E. The asterisk marks the point $k = 1.3$, $\theta_E = 9$. (c) Growth-rate of the most unstable eigenmode obtained from stability analysis of the time-averaged zonal flow shown in Fig. 4a. The diagram is constructed by multiplying the vertical shear profile by the constant m_0. Statistical equilibrium corresponds to $k = 1.3$, $m_0 = 1$, and is denoted by an asterisk. Contour interval is 0.1.

is confined to the tropical region; this is not surprising since we are dealing with quite a short wave (zonal wavenumber 6). We do not take these details of our model seriously, however, since in any case it describes an incorrect tropical dynamics.

Several theories on midlatitude influence (teleconnections) of anomalous tropical heating are based on the computation of flow anomalies with respect to *static* "basic states" identified with time-mean flows either of GCMs or of the real atmosphere (see, for example, Simmons 1982). In Fig. 11, we show the results of a

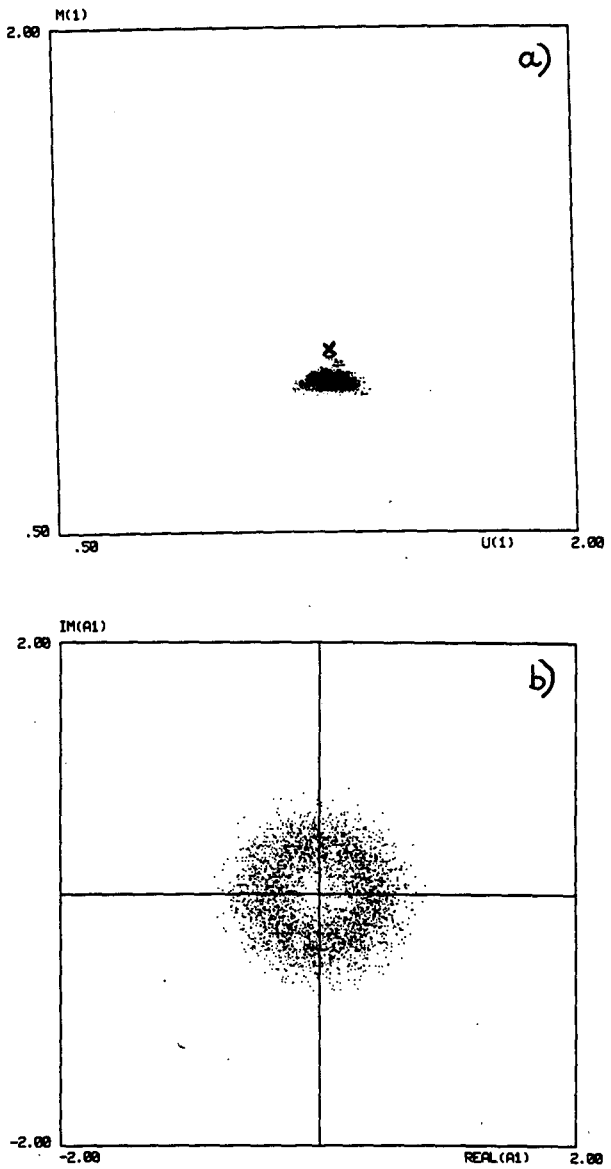

FIG. 8. Scatter diagram of (a) zonal wind and (b) first barotropic wave-component for the system with external forcing producing a fixed point at the statistical equilibrium. A cross marks the position of the old statistical equilibrium. Compare with Fig. 2.

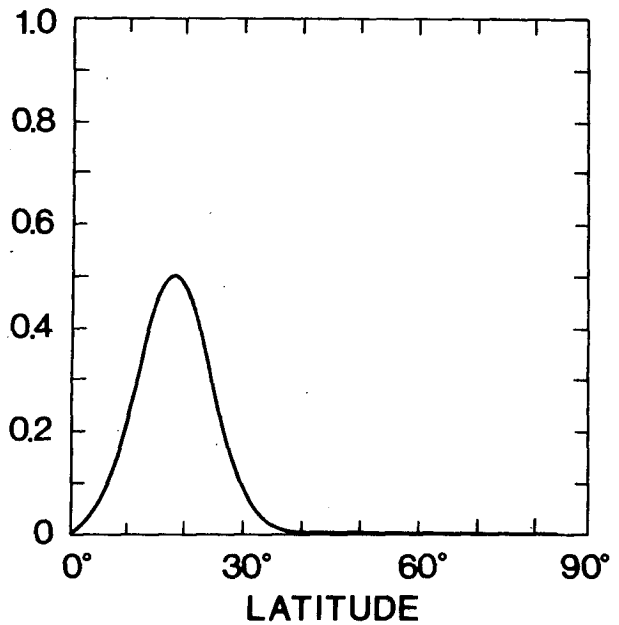

FIG. 9. Latitudinal structure of the heat source H[see text, Eq. (17)] used in the numerical experiment described in section 4.

linear calculation performed along such lines with the same parameters of the numerical simulation described above. The equations of motion are linearized around the time-mean state shown in Fig. 4a and the stationary solution forced by the anomalous heating (12) is computed. Inspection of the linear solution and comparison with the results of direct numerical simulation (Fig. 10) shows that the two have nothing in common, except latitudinal confinement (associated with the short longitudinal scale of the heat-source).

The reason for the above differences should now be clear: as shown previously, the time-mean state of a chaotic system carries no dynamic information concerning free fluctuations; we have also shown that the same holds for forced anomalies.

5. The model atmosphere as a dynamical system

The first approach proposed herein to interpreting the dynamics of our model atmosphere is typical of the theory of dynamical systems; the idea is to follow the onset of turbulent chaos by varying a macroscopic state parameter, in our case the external thermal forcing.

A stationary solution is most easily determined as the "Hadley circulation":

$$\left.\begin{aligned} &A = B = 0 \\ &U = m \\ &\nu_S m_{yy} - 2F\nu_H(m - m^*) = 0 \end{aligned}\right\} \qquad (13)$$

which is characterized by zero wind in the lower layer. Linear stability analysis of this solution gives the results already shown in Fig. 7 for the first and second most unstable modes.

For $k = 1.3$ stability is lost around $\theta_E = 4.16$. Figure 12 illustrates the bifurcation sequence. At $\theta_E = 4$ the system is stable; the stable orbit, at $\theta_E = 4.07$, is winding several times before spiraling down to equilibrium, and degenerating at $\theta_E = 4.2$ into a stable Hopf cycle. Between 4.2 and 4.3, another cycle is bifurcated; the motion looks quasiperiodic, i.e., the ratio between the period of the new orbit and that of the first Hopf cycle is irrational and the ensuing vacillation covers its toroidal phase space. At high values of forcing, the whole space near statistical equilibrium is filled. The sequence seems to be the type described by Feigenbaum et al. (1982) who also provide an example of renormalization near the transition to chaos.

Stable and unstable orbits or vacillations can be determined for the truncated version of (8)–(11) by standard procedures. Periodic orbits (which are fixed points in U and m) are born at Hopf bifurcations of the Hadley circulation and can be followed by a modified version of the Newton–Keller continuation algorithm (see Kubícek and Marek 1983). Figure 13 shows the bifurcation diagram relative to system (8)–(11) obtained for two different truncations ($JT = 16$ and $JT = 32$). None of these orbits (which are sometimes referred to as Rossby circulations) reaches a meaningful radius for $\theta_E = 9$. In particular, the orbit born at the first Hopf bifurcation ($\theta_E = 4.158$) soon loses its stability in a saddle node bifurcation near $\theta_E = 4.2$; at this point the geopotential associated with the wave reaches only a few meters (see Fig. 12c).

Along each particular periodic orbit several Hopf bifurcations occur where vacillations are born. Vacillations are characterized by U and m periodic and A and B quasi-periodic in time; they are found by searching for the fixed point of the return map (see Sparrow 1982). In Fig. 13 one vacillation is followed (the least expensive to compute, although it is the most interesting as it is created where the first Rossby circulation loses its stability) to show that several additional bifurcations can be found at which either period-doubling occurs or quasi-periodic orbits characterized by three frequencies are created (see, for instance, Kubícek and Marek 1983, pp. 222–223).

It appears evident that the number of quasi-periodic or periodic orbits increases dramatically by penetrating more and more deeply into the unstable region. Since the prototype of atmospheric behavior we are interested in is far from transitional, there is not much quantitative knowledge we can gain from the study of the bifurcation sequence.

A second line of approach is tried, which consists in studying different embeddings of the attractor on different Fourier truncations of system (8)–(11). Trun-

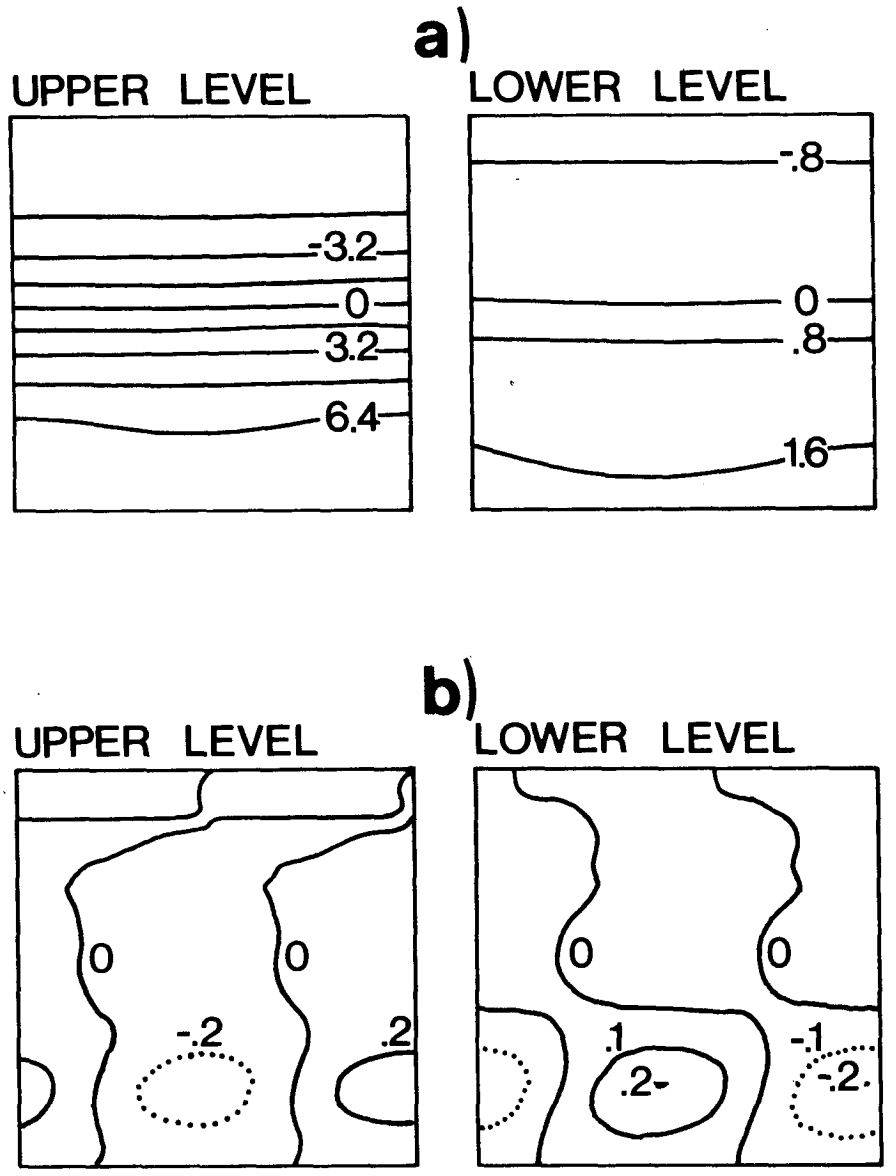

FIG. 10. Ten year average of (a) total streamfunction field, and (b) deviation from zonal mean (anomaly) plotted at the two levels 1 and 3 (see section 4). Contour intervals are (a) 160 m and 80 m of geopotential height for the total field at upper and lower level, and (b) 20 m and 10 m of geopotential height for the anomaly field at the upper and lower level, respectively.

cation has, to a certain extent, the same qualitative effects as the decrease of the stress parameter: if the dimension of the truncated space is not sufficient for the embedding of the center manifold of the instability "generating" the chaos, the system is stabilized. However, the spectra of Fig. 6 substantiate the hypothesis that, at least energetically, a limited number of components plays a dominant role. It is interesting, therefore, to consider the phenomenology of a sequence of truncations in analogy with the sequence of bifurcations discussed above. Figure 14 shows the results which apply to three cases: $(i, j) = (4, 4)$, $(8, 4)$ and $(8, 8)$ where i is the number of Fourier modes in the zonal flow and j is the number of modes in the wave field. The diagram is relative to the phase space projection onto the lowest modes of the zonal flow U and m. The fixed point of the (4, 4) system, strongly shifted with respect to the Hadley circulation because of the extreme efficiency of the waves in transporting momentum and heat, becomes a stable, though less efficient, cycle for

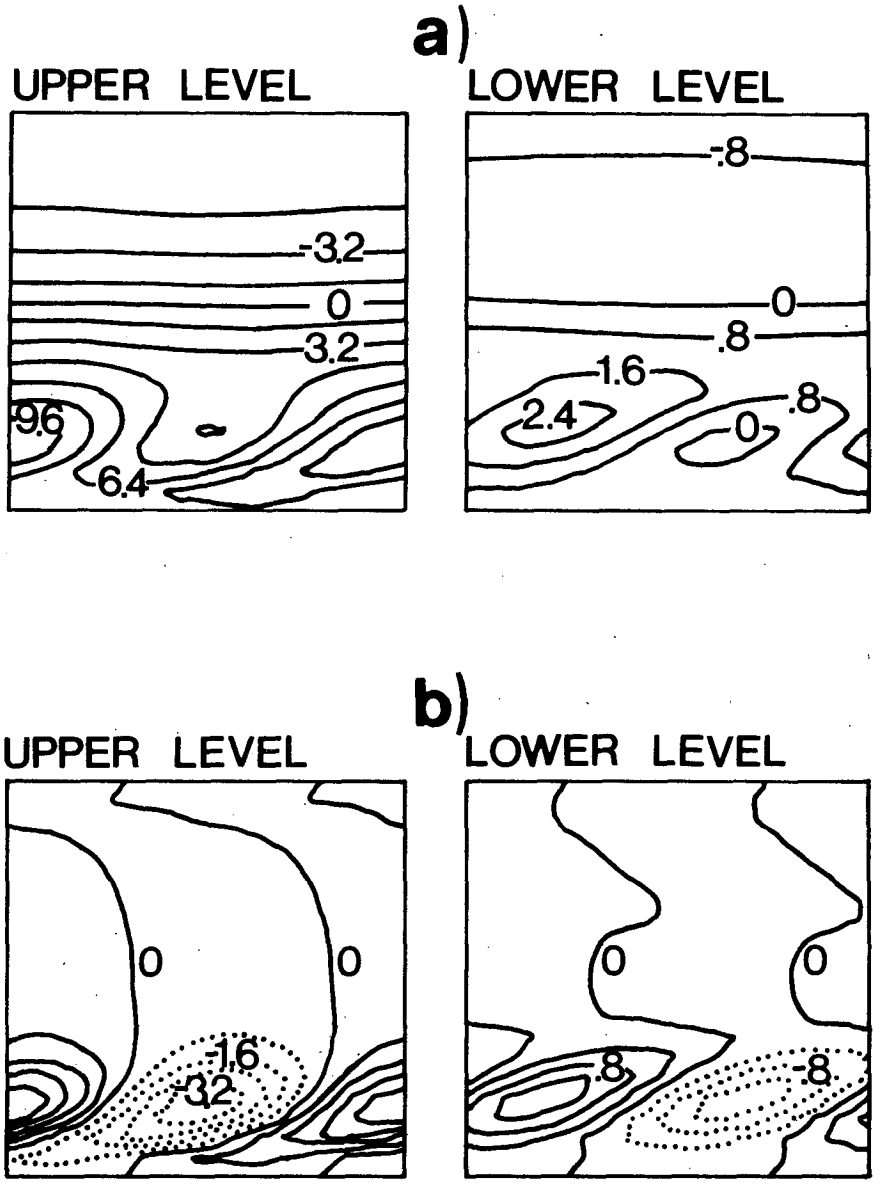

FIG. 11. Stationary, linear response of system (8)–(11) to the heat source shown in Fig. 9. As in Fig. 10 but contour interval of anomaly field is 80 m and 40 m of geopotential height at upper and lower level, respectively.

the (8, 4) system. As already pointed out, we improperly use the term of "cycle", because in the rest of the phase-space, the orbits are ergodic and filling (vacillations of waves are characterized by irrational period ratio). Comparison of the scatter diagram of the zonal flow in the (8, 8) system with the original one (in Fig. 2) shows that the cloud of points has practically the same extension as in the high-resolution run. Furthermore, the variance seems very well distributed around the (8, 4) cycle, suggesting the possibility that the attractor be "born" out of the instability of such a new "basic state". Unfortunately, the (8, 4) cycle is not an exact solution of the complete system: instead of resorting to instability analysis we thus introduce new degrees of freedom perturbatively on the (8, 4) system. In the Appendix we show how this is done.

As far as the instability of more complex basic states is concerned, an adequate discussion of the physical mechanism that is at the basis of such behavior requires careful mathematical consideration regarding the properties of instabilities growing on periodic and quasi-periodic orbits versus those growing on fixed

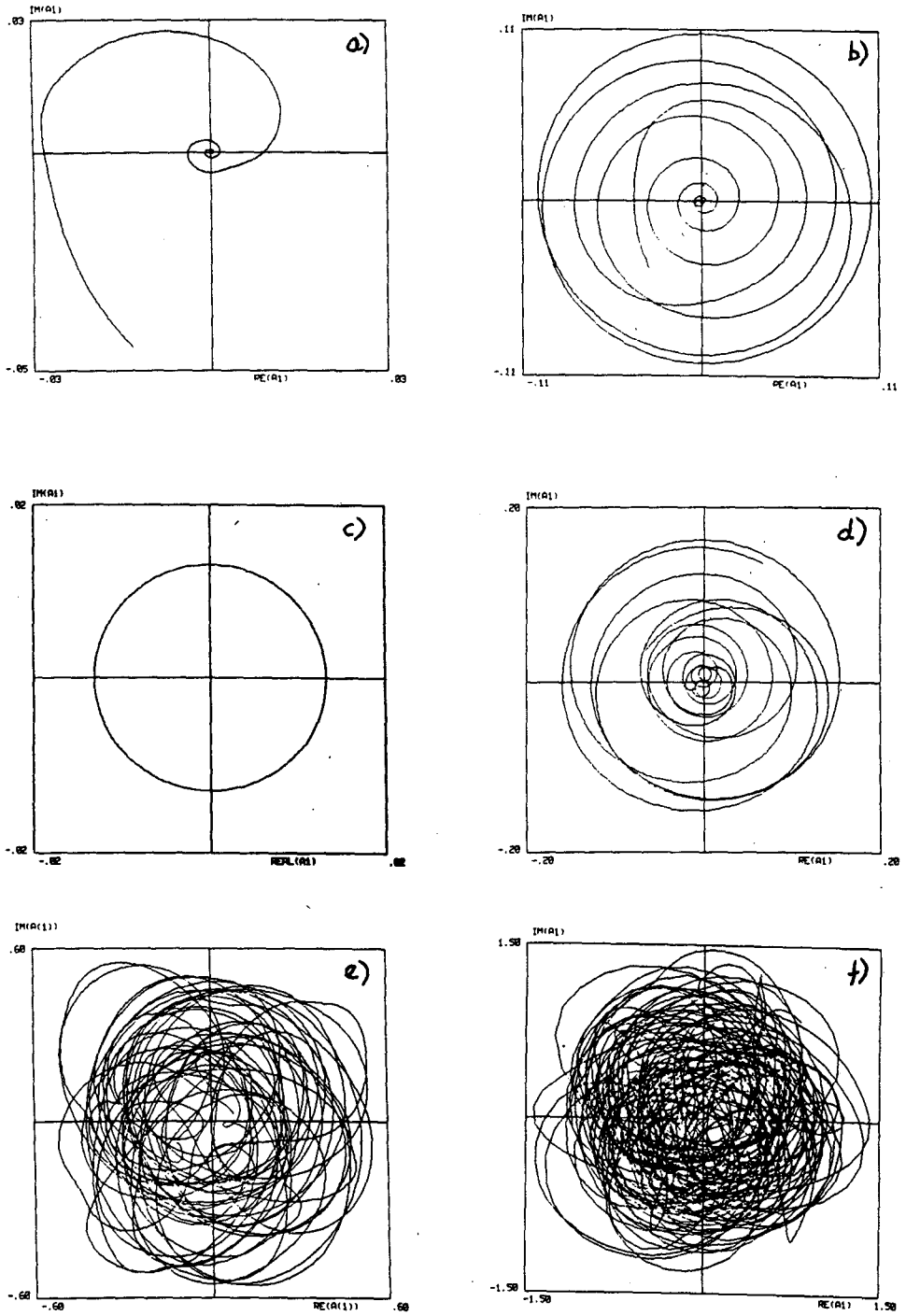

FIG. 12. Projection of the phase-space trajectory on the $(\mathrm{Im}(A_1), \mathrm{Re}(A_1))$ plane for different values of the external forcing. All the trajectories describe a 1-yr evolution of the system. (a) $\theta_E = 4$, (b) $\theta_E = 4.07$, (c) $\theta_E = 4.2$, (d) $\theta_E = 4.3$, (e) $\theta_E = 6$, and (f) $\theta_E = 9$. The Hadley circulation loses its stability at $\theta_E \approx 4.158$. Note that the dimension of the attractor expands with growing θ_E.

points centered on the time average. Suffice it here to remark that many properties are extremely different. Therefore, we may have a potential explanation of the discrepancies between the classical theory of baroclinic instability and available observations. Moreover, if the global properties of phase-space of the baroclinic system

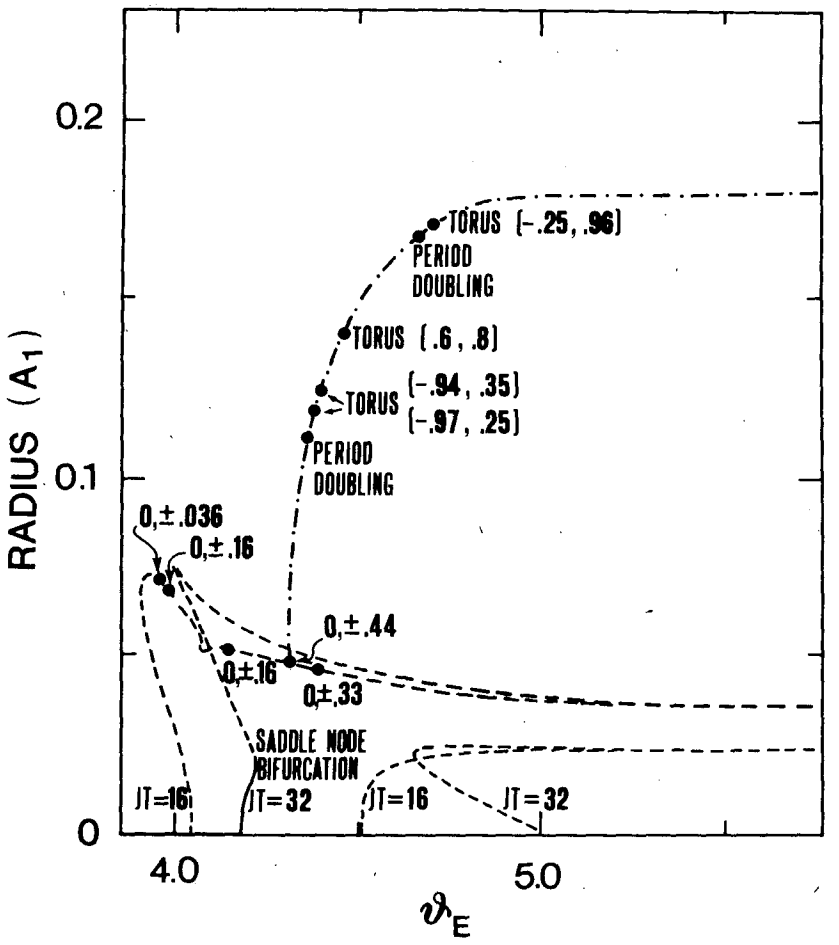

FIG. 13. Bifurcation diagram of system (8)–(11) obtained for two different truncations of the Fourier expansion (16 and 32 modes). The abscissa gives the stress parameter while the y-axis indicates the amplitude in meters of the first Fourier component of the barotropic wave field (A_1). In the case of quasi-periodic orbits (dashed–dotted line) the curve gives the maximum amplitude reached in the vacillation cycle. Continuous lines refer to stable Rossby circulations, broken lines to unstable ones. The numbers between parentheses are the eigenvalues of the stability analysis at Hopf bifurcations (marked by a dot). Numbers between square brackets are Floquet multipliers lying on the unit circle, where new quasi-periodic orbits are born.

are associated with the instability of a basically cyclic process, the identification of such a process in the real atmospheric circulation becomes a primary task. At this point, an obvious hypothesis is that the indicial circulation may be more "fundamental" than previously thought. These problems are the subject of an ongoing investigation.

6. Conclusions

Given the importance of the mechanism of maintenance of statistical equilibrium of baroclinic turbulence in the atmosphere, we hesitate to state any firm conclusion; much more work is needed on the statistical properties of various model atmospheres and, even more, on similar properties of the observed atmospheric circulation.

In this work we have reexamined some of the concepts that are at the basis of the theory of general circulation and, in particular, the theory of ordinary baroclinic instability. Particular attention has been paid to the classical scheme that describes the interaction between nonsymmetric disturbances and zonal circulation in terms of properties of unstable eigenmodes of the linear stability of the time-averaged flow. The dangers involved in this approach are exemplified in the numerical experiment shown in section 4. In particular, such eigenmodes by carrying heat poleward, produce a new shift toward marginal stability of the time-mean zonal wind. Our conclusion is that the time-mean state carries no information about the dynamics of fluctuations around it.

The question of signal propagation in random media has been pursued by showing that, in the problem of

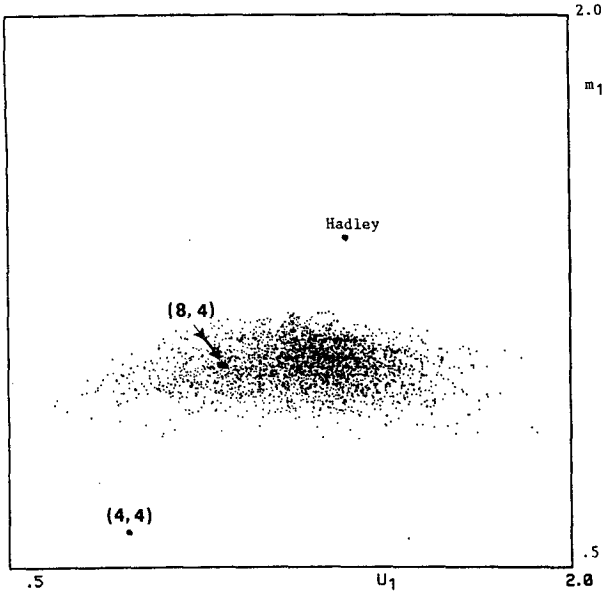

FIG. 14. Scatter diagram in the (U_1, m_1) plane showing the position of the stable fixed point obtained in the (4, 4) simulation, the stable orbit in the (8, 4) case and the chaotic attractor in the (8, 8) case. Also reported is the position of the Hadley circulation.

determining anomalies due to tropical heating, the linear response of the time-mean state can be very different from the time-averaged response of the system. In this connection, it will be interesting to compute in our model the time-mean of the response obtained by linearizing around each single instantaneous state of the unforced problem. This computation may suggest a simple statistical model which is capable of providing a better estimation of the real atmospheric response to anomalous external forcing than the classical one. Work along these lines is in progress; however, it is clear that a thorough investigation of the problem of teleconnections between anomalous tropical heating and midlatitude circulation requires the use of a general circulation model. The simple model we have used is limited in many respects; e.g., the fact that the midlatitude response is very small due to the relatively short wavelength of the most unstable baroclinic wave.

Acknowledgments. The computer time needed to complete this work has been made available by the "Program for the Use of Large Vector Computers" of the CINECA (Centro di Calcolo Inter-universitario dell'Italia Nord-Orientale) of Bologna.

APPENDIX

Lower Order Models

Among all possible severely truncated versions of system (8)–(11), the one with four Fourier modes in the wave fields A, and B and eight Fourier components in the zonal fields U, and m gives a simple, quasi-periodic attractor which, more than any other simple, stable orbit with few degrees of freedom, is centered near the maximum frequency state of the original sys-

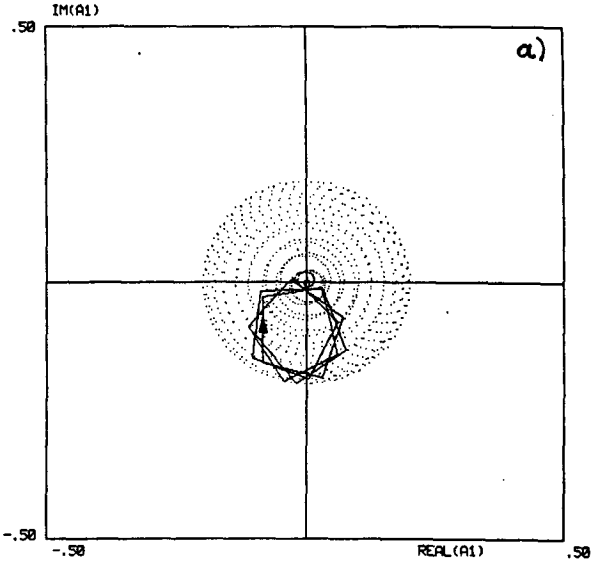

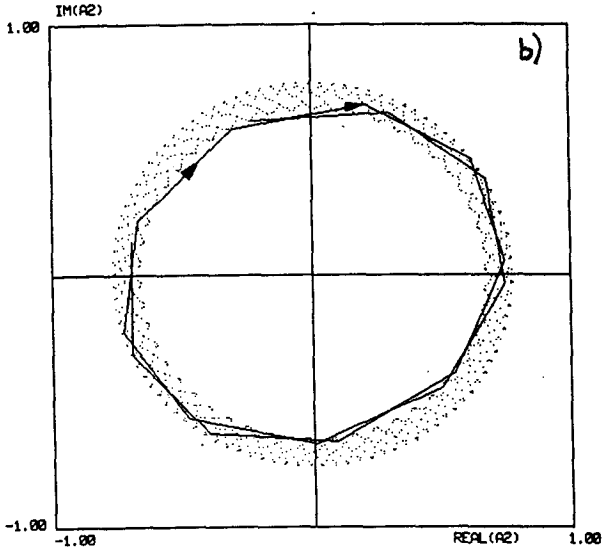

FIG. 15. (a) Projection of the vacillation obtained with the (8, 4) system (see text) in the $\mathrm{Re}(A_1)$, $\mathrm{Im}(A_1)$ plane. Total time of integration is 800 units; one point every 0.5 unit is plotted. The continuous, broken line represents the trajectory described in 8 time units and gives an idea of how the phase space is filled. Part (b) as in (a), except for the second barotropic wave component A_2.

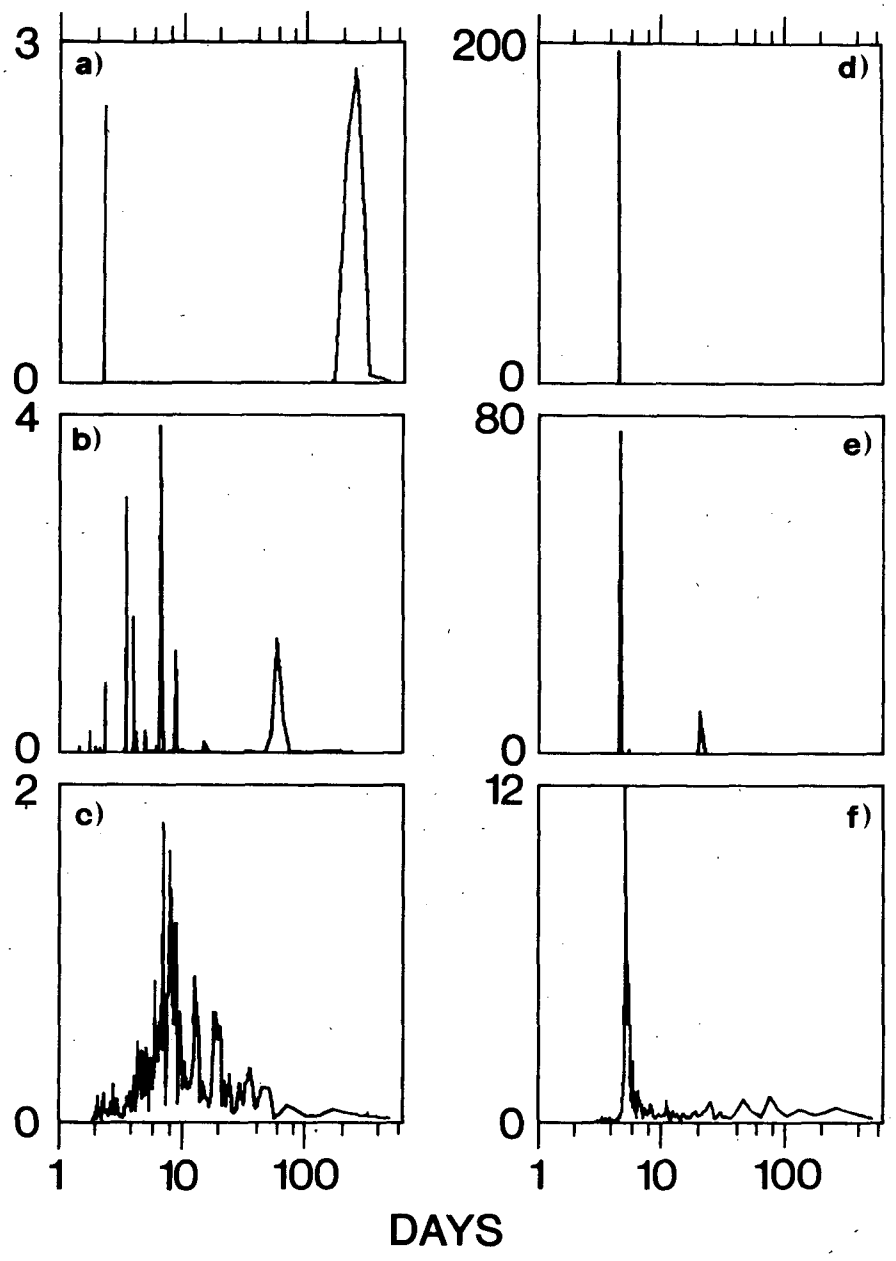

FIG. 16. (a) Power spectrum of the real part of A of the vacillation shown in Fig. 14 and Fig. 15. The abscissa reports the period on a logarithmic scale. (b) As in (a) but with $\epsilon = 0.1$. (c) As in (a) except $\epsilon = 0.4$. (d), (e), (f) As in (a), (b), (c) except for the real part of A_2.

tem (8)–(11). Figure 15 shows some other projections in the phase space of the vacillation obtained with the (8, 4) system.

At this point, we asked whether chaos develops gradually out of this orbit, as occurs in conservative systems, by inserting perturbatively the remaining degrees of freedom (KAM tori), eventually filling the phase space near statistical equilibrium. Figure 16a–f shows the power spectrum of two time series, the real part of A_1 and the real part of A_2, obtained respectively for $\epsilon = 0$, 0.1, and 0.4. Here, ϵ is the perturbative parameter by which the degrees of freedom are multiplied for other than those of the (8, 4) system. The power spectrum of the same variables in the original system ($\epsilon = 1$) are shown in Fig. 5a, b. For $\epsilon = 0.4$ the (8, 4) orbit, which is basically a cycle in the *antisymmetric* wave components, is clearly still recognizable superimposed on a continuum of frequencies. Between

$\epsilon = 0$ and 0.1, new frequencies appear (see Fig. 16a, b), indicating the existence of bifurcations at which new quasi-periodic orbits (but still very similar to the original one) are born.

Nevertheless, comparison with the power spectrum of the high resolution run (Fig. 5) shows that between $\epsilon = 0.4$ and 1 the strong peak around 5.5 days of the period (Fig. 16f) is absorbed into the continuous background of frequencies. On the other hand, the power spectrum at $\epsilon = 1$ suggests the presence of a cycle in the *symmetric* wave components, with a period of about 4 days. The existence of an unstable, quasi-periodic orbit having these characteristics could not be demonstrated, however, due to the numerical difficulties involved.

REFERENCES

Defant, A., 1921: Die zirkulation der atmosphare in den gemassigten breiten der erte. *Geograf. Ann.*, **3**, 209–266.

Douglas, C. K. M., 1931: A problem of the general circulation. *Q. J. Roy. Meteor. Soc.*, **57**, 423–431.

Farmer, J. D., 1982: Chaotic attractors of an infinite-dimensional dynamical system. *Physica*, **4D**, 366–393.

Feigenbaum, M. J., L. P. Kadanoff, and S. J. Shenker, 1982: Quasi-periodicity in dissipative systems: A renormalization group analysis. *Physica D*, **3**, 370–386.

Frederiksen, J. S., 1978: Growth rates and phase speeds of baroclinic waves in multi-level models on a sphere. *J. Atmos. Sci.*, **35**, 1816–1826.

Hart, J. E., 1979: Finite amplitude baroclinic instability. *Ann. Rev. Fluid Mech.*, **11**, 147–172.

Hoskins, B. J., 1983: Large-scale dynamical processes in the atmosphere. Academic Press,

Hussain, A. K. M. F., 1983: Coherent structures—reality and myth. *Phys. Fluids*, **26**(10), 2816–2850.

Jeffreys, H., 1926: On the dynamics of geostrophic winds. *Q. J. Roy. Meteor. Soc.*, **52**, 85–104.

Kubícek, M., and M. Marek, 1983: Computational methods in bifurcation theory and dissipative structures. Springer-Verlag,

Lorenz, E. N., 1963: The mechanism of vacillation. *J. Atmos. Sci.*, **20**, 448–464.

——, 1967: The nature and theory of the general circulation of the atmosphere W.M.O.

Pedlosky, J., 1970: Finite amplitude baroclinic waves. *J. Atmos. Sci.*, **27**, 15–30.

——, 1979: Geophysical fluid dynamics. Springer-Verlag.

Saltzman, B., 1968: Steady state solutions for axially symmetric climatic variables. *Pure Appl. Geophys.*, **69**, 237–259.

——, 1978: A survey of statistical–dynamical models of the terrestrial climate. *Adv. Geophys.*, **20**, 183–304.

——, and A. D. Vernekar, 1968: A parameterization of the large scale eddy flux of relative angular momentum. *Mon. Wea. Rev.*, **96**, 854–857.

——, and ——, 1971: An equilibrium solution for the axially symmetric component of the Earth's macroclimate. *J. Geophys. Res.*, **76**, 1498–1524.

Simmons, A. J., 1982: The forcing of stationary wave motion by tropical diabatic heating. *Quart. J. Roy. Meteor. Soc.*, **108**, 503–534.

——, and B. J. Hoskins, 1978: The life cycles of some nonlinear baroclinic waves. *J. Atmos. Sci.*, **35**, 414–432.

Sparrow, C., 1982: *The Lorenz Equations: Bifurcations, Chaos, and Strange Attractors.* Springer-Verlag.

Speranza, A., and P. Malguzzi, 1986: The response of atmospheric circulation to anomalous tropical heating: a re-examination of the theory of teleconnections in the context of turbulence theory. Study week: "Persistent Meteo-Oceanographic Anomalies and Teleconnections", Rome.